Journal Pre-proofs

Review

A high-throughput, multi-index isothermal amplification platform for rapid detection of 19 types of common respiratory viruses including SARS-CoV-2

Wanli Xing, Yingying Liu, Huili Wang, Shanglin Li, Yongping Lin, Lei Chen, Yan Zhao, Shuang Chao, Xiaolan Huang, Shaolin Ge, Tao Deng, Tian Zhao, Baolian Li, Hanbo Wang, Lei Wang, Yunpeng Song, Ronghua Jin, Jianxing He, Xiuying Zhao, Peng Liu, Weimin Li, Jing Cheng

PII: S2095-8099(20)30238-1
DOI: https://doi.org/10.1016/j.eng.2020.07.015
Reference: ENG 502

To appear in: *Engineering*

Received Date: 21 April 2020
Revised Date: 28 June 2020
Accepted Date: 21 July 2020

Please cite this article as: W. Xing, Y. Liu, H. Wang, S. Li, Y. Lin, L. Chen, Y. Zhao, S. Chao, X. Huang, S. Ge, T. Deng, T. Zhao, B. Li, H. Wang, L. Wang, Y. Song, R. Jin, J. He, X. Zhao, P. Liu, W. Li, J. Cheng, A high-throughput, multi-index isothermal amplification platform for rapid detection of 19 types of common respiratory viruses including SARS-CoV-2, *Engineering* (2020), doi: https://doi.org/10.1016/j.eng.2020.07.015

Research
Coronavirus Disease 2019—Review

A High-Throughput, Multi-Index Isothermal Amplification Platform for Rapid Detection of 19 Types of Common Respiratory Viruses Including SARS-CoV-2

Wanli Xing [a,b,c,#], Yingying Liu [b,d,#], Huili Wang [e,#], Shanglin Li [a,#], Yongping Lin [f], Lei Chen [g], Yan Zhao [h], Shuang Chao [i], Xiaolan Huang [j], Shaolin Ge [b,d], Tao Deng [c], Tian Zhao [b,d], Baolian Li [b,d], Hanbo Wang [b,d], Lei Wang [b,d], Yunpeng Song [c], Ronghua Jin [k], Jianxing He [l], Xiuying Zhao [m], Peng Liu [a,*], Weimin Li [n,*], Jing Cheng [a,b,d,*]

[a] *Department of Biomedical Engineering, School of Medicine, Tsinghua University, Beijing 100084, China*

[b] *National Engineering Research Center for Beijing Biochip Technology, Beijing 102206, China*

[c] *CapitalBio Technology, Beijing 101111, China*

[d] *CapitalBio Corporation, Beijing 102206, China*

[e] *Department of Basic Medical Sciences, School of Medicine, Tsinghua University, Beijing 100084, China*

[f] *Department of Laboratory Medicine, First Affiliated Hospital of Guangzhou Medical University, Guangzhou 510120, China*

[g] *Department of Neurology, West China Hospital, Sichuan University, Chengdu 610041, China*

[h] *Clinical Laboratory Center, Beijing Youan Hospital, Capital Medical University, Beijing 100069, China*

[i] *Department of Pediatrics, Beijing Tsinghua Changgung Hospital, School of Clinical Medicine, Tsinghua University, Beijing 102218, China*

[j] *Experiment Center, Capital Institute of Pediatrics, Beijing 100020, China*

[k] *President's Office, Beijing Youan Hospital, Capital Medical University, Beijing 100069, China*

[l] *Department of Cardiothoracic Surgery, The State Key Laboratory of Respiratory Disease, China Clinical Research Center for Respiratory Disease, Guangzhou Institute of Respiratory Health, First Affiliated Hospital of Guangzhou Medical University, Guangzhou 510120, China*

[m] *Department of Clinical Laboratory, Beijing Tsinghua Changgung Hospital, School of Clinical Medicine, Tsinghua University, Beijing 102218, China*

[n] *Department of Respiratory and Critical Care Medicine, West China Hospital, Sichuan University, Chengdu 610041, China*

* Corresponding authors.

E-mail addresses: pliu@tsinghua.edu.cn (P. Liu), weimin003@163.com (W. Li), jcheng@tsinghua.edu.cn (J. Cheng).

[#] These authors contributed equally as the first authors of this work.

ARTICLE INFO

Article history:
Received 21 April 2020
Revised 28 June 2020
Accepted 21 July 2020
Available online

Keywords:
Coronavirus disease 2019
Severe acute respiratory syndrome coronavirus 2
Microfluidics
Nucleic acid testing
Isothermal amplification

ABSTRACT

Fast and accurate diagnosis and the immediate isolation of patients infected with severe acute respiratory syndrome coronavirus 2 (SARS-CoV-2) are regarded as the most effective measures to restrain the coronavirus disease 2019 (COVID-19) pandemic. Here, we present a high-throughput, multi-index nucleic acid isothermal amplification analyzer (RTisochip^{TM}-W) employing a centrifugal microfluidic chip to detect 19 common respiratory viruses, including SARS-CoV-2, from 16 samples in a single run within 90 min. The limits of detection of all the viruses analyzed by the RTisochip^{TM}-W system were equal to or less than 50 copies per microliter, which is comparable to those of conventional reverse-transcription polymerase chain reaction. We also demonstrate that the RTisochip^{TM}-W system possesses the advantages of good repeatability, strong robustness, and high specificity. Finally, we analyzed 201 cases of preclinical samples, 14 cases of COVID-19-positive samples, 25 cases of clinically diagnosed samples, and 614 cases of clinical samples from patients or suspected patients with respiratory tract infections using the RTisochip^{TM}-W system. The test results matched the referenced results well and reflected the epidemic characteristics of the respiratory infectious diseases. The coincidence rate of the RTisochip^{TM}-W with the referenced kits was 98.15% for the detection of SARS-CoV-2. Based on these extensive trials, we believe that the RTisochip^{TM}-W system provides a powerful platform for fighting the COVID-19 pandemic.

1. Introduction

The coronavirus disease 2019 (COVID-19) pandemic, which is caused by severe acute respiratory syndrome coronavirus 2 (SARS-CoV-2), is quickly spreading throughout the world [1]. As of 26 June 2020, despite the rigid restrictions adopted by many countries worldwide, over 9.47 million total confirmed cases of COVID-19 have been reported in 188 countries and territories, resulting in approximately 0.48 million deaths. Since there are no effective drugs or vaccines for COVID-19 as yet, the rapid diagnosis and isolation of patients infected with SARS-CoV-2 have been regarded as the most effective way to restrain the ongoing pandemic. Unfortunately, COVID-19 shares many common symptoms with the flu and cold, such as fever, dry cough, and myalgia or fatigue [2]. As a result, reliable diagnostic tools for differentiating the novel coronavirus from other common respiratory viruses are greatly desired in the fight against COVID-19. So far, a variety of nucleic acid testing kits based on reverse-transcription polymerase chain reaction (RT-PCR) have been developed and are playing a central role in clinically diagnosing COVID-19 [3,4]. However, these RT-PCR kits are usually time-consuming, can only detect SARS-CoV-2, and occasionally produce false-negative results due to either sampling or sensitivity issues. In clinical practice, SARS-CoV-2-negative patients tested by RT-PCR with persistent COVID-19-like symptoms can still consume a great deal of precious medical resources and have a high risk of cross-infection if treated inappropriately. Therefore, it is extremely urgent to develop a diagnostic tool that can not only rapidly detect SARS-CoV-2, but also accurately identify other common respiratory viruses, such as influenza viruses, human parainfluenza virus (HPIV), and so forth [5–7], so that the exact cause of the symptoms can be known when the SARS-CoV-2 test is negative.

Multiplex RT-PCR is capable of detecting several types of viruses by mixing all the primers in a single tube. However, due to the inevitable interferences of these mixed primers and the limited number of available fluorophores for detection, the development of a robust multiplex system is extremely difficult and the number of detected targets is generally limited to less than ten per reaction [8]. One of the most promising methods for breaking this limitation is to transform a multiplex polymerase

chain reaction (PCR) into a multiple single-plex PCR by physically isolating different primer pairs into designated compartments. In the past decades, microfluidic technology has become one of the most common methods to realize the sample partitioning strategy without introducing additional manual operations. Among various microfluidic technologies, such as hydrophilic–hydrophobic patterning [9,10], the SlipChip [11–14], and electrowetting-on-dielectric (EWOD) technology [15,16], the centrifugal-based method offers the advantages of simple operations, fully enclosed microstructures, and easy integration with other microfluidic functions [17,18]. Our group previously developed a disc-shaped centrifugal microdevice operated in a compact instrument with a single channel (only one sample tested per run) and proved the excellent multiplexing capability of this system by demonstrating the detection of 13 respiratory pathogenic bacteria using loop-mediated isothermal amplification (LAMP) on a single chip [19]. However, when viruses are detected, neither RT-PCR nor LAMP are amenable for use with a microchip due to thermal cycling and primer design problems, respectively. Several other microfluidic systems, including FilmArray® and Verigene®, have also been invented for multiplex pathogen detection and have the advantages of integration with sample preparations [20–22]. Unfortunately, no microfluidic systems have been reported as yet for distinguishing SARS-CoV-2 from other respiratory viruses.

Nucleic acid sequence-based amplification (NASBA) is an enzyme-based isothermal amplification method that employs a mixture of reverse transcriptase, ribonuclease (RNase) H, T7 ribonucleic acid (RNA) polymerase, two specially designed primers, and a specially designed probe [23,24]. In the initial-reaction phase of NASBA, primer 1 anneals to the single-stranded RNA, synthesizes the complementary deoxyriboNucleic acid (cDNA), and forms an RNA:DNA hybrid. Subsequently, RNase H hydrolyzes the RNA chain and generates single-stranded DNA. After annealing with primer 2, reverse transcriptase synthesizes double-stranded DNA with a promoter region that can be recognized by T7 RNA polymerase [23,24]. Once the double-stranded DNA with a promoter region is generated, the reaction enters into continuous cycles of transcription, reverse transcription, and hydrolysis of the RNA in the RNA:DNA hybrid [23–25]. Since 10–1000 copies of RNA can be generated in each step of transcription, the NASBA process requires fewer cycles than PCR or LAMP, which reduces the total incubation time and overall error frequency [23,26]. As an isothermal amplification method, NASBA is robust, specific, and particularly suitable for the detection of single-stranded RNA, although it is not fit for double-stranded DNA [23,27].

In the current study, we demonstrate the development of a high-throughput, multi-index nucleic acid isothermal amplification analyzer (RTisochip™-W) based on our disc-shaped centrifugal microfluidic technology with two major improvements. First, we chose NASBA, which is an efficient and sensitive isothermal RNA amplification technique [23,26,28,29], to replace the incompatible PCR and LAMP for detecting viruses in the centrifugal microchip. Second, we designed an array of 16 single-channel sub-modules, which were updated from the previous single-channel instrument, to increase the throughput of the system. As a result, this brand-new RTisochip™-W system is capable of detecting 19 common respiratory viruses, including SARS-CoV-2, from 16 clinical samples in a single run within 90 min. The excellent performance of our system, which is proved by the thorough characterization in the current study, prompts us to envision this RTisochip™-W system as playing a critical role in fighting the COVID-19 pandemic.

2. Materials and methods

2.1. Sample collections and RNA extractions

Plasmids containing the targeted virus sequences were synthesized by Sangon Biotech (Shanghai) Co., Ltd. RNA templates were prepared by *in vitro* transcription using a HiScribe™ T7 High-Yield RNA Synthesis Kit (New England BioLabs, USA) according to the manufacturer's instructions. All the inactivated virus culture stocks were given as a gift by Dr. Nanshan Zhong from the First Affiliated Hospital of Guangzhou Medical University. Clinical samples were collected with the patients' informed consent from the Beijing Tsinghua Changgung Hospital, the Capital Institute of Pediatrics, the First Affiliated Hospital of Guangzhou Medical University, the West China Hospital of Sichuan University, and the Beijing Youan Hospital of Capital Medical University during the period of 2018–2020.

Throat swab samples were collected with a DNA flocked swab (93050, Miraclean Technology Co., Ltd., China) by rotating the swab tip in the throat to collect the cellular material; the swab was then placed into virus transport medium (MT0301, Youkang Hengye Biotechnology (Beijing) Co., Ltd., China). After the swab tip was immersed in the virus transport medium for a few seconds, the end of the swab tip was broken and the sample was maintained at –70 °C for long-term storage.

The total RNA from the clinical samples was extracted using TRIzol™ Reagent (Invitrogen, USA) or a QIAamp® Viral RNA Mini Kit (Qiagen, Germany) following the manufacturers' instructions. Automated RNA extraction was performed with the KingFisher™ Flex Purification System (Thermo Fisher Scientific, USA) according to the user's operation manual. The extracted RNA was dissolved in RNase-free water and quantified using a Nanodrop 2000 or Qubit 3.0 (all from Thermo Fisher Scientific, USA). The integrity of the RNA was examined using 1% formaldehyde denaturing gel electrophoresis.

2.2. Primer design and NASBA reactions

The common respiratory viruses that can be detected by our system include SARS-CoV-2 (S and N genes), influenza A (H1N1, H1N1 2009, H3N2, H7N9), influenza B, respiratory syncytial virus (RSV), human metapneumovirus (HMPV), HPIV1, HPIV2, HPIV3, HPIV4, human rhinovirus (HRV), enterovirus 71 (EV71), coxsackievirus A16 (CA16), coxsackievirus A6 (CA6), human coronavirus (HCoV)-229E/NL63, and HCoV-OC43/HKU1. NASBA, an isothermal amplification technology, was employed for the on-chip detection of viral RNAs. The NASBA primers and probes were designed using the Primer Premier v.5.0 software (Premier Biosoft, USA) and synthesized by Sangon Biotech (shanghai) Co., Ltd., China. The sequences of primers and probes are listed in Table S1 of Appendix A. We also performed coverage analysis of the primers and probes of each pathogen; the results are listed in Supplementary data 2 of Appendix A. We downloaded ten recently published complete whole genome sequences of each pathogen to perform the coverage analysis. On the whole, the primers and probes designed in our system have very good coverage. For example, for H1N1 2019, the primers and probes totally matched with ten recently published complete whole genome sequences, indicating that the region we chose for primer and probe design is very conservative.

In the on-chip NASBA assay, a total of 1 μL of the home-made spotting solution containing each set of primers and probes was pipetted into each corresponding reaction chamber and dried completely at room temperature. During the analysis, a total of 55

μL of the total NASBA mixture containing 16.5 μL of the buffer solution, a total of 13 μL of Nucleoside triphosphate (NTP) solution, 5.5 μL of the enzyme mix (all from CapitalBio Technology, China), and 20 μL of RNA template were mixed in a tube and then injected into the chip with a pipette.

2.3. Design and operation of the microfluidic chip

The microfluidic chip for the detection of 19 types of respiratory viruses has been reported previously by our group [30,31]. In brief, as illustrated in Fig. 1(a), the disc-shaped microfluidic chip has a diameter of 62 mm and a thickness of 0.6 mm; it is comprised of a structural layer and a thin cover layer connected by double-sided adhesive tape. The structural layer contains 24 reaction chambers (each 3 mm in diameter and 0.2 mm in depth) with a volume of 1.45 μL each, 24 buffer cells, a sine-shaped main channel (0.2 mm in width and 0.1 mm in depth), an inlet, and an outlet. Each reaction chamber is connected to the main channel via a buffer cell and a short pipe. The structural layer was fabricated of polycarbonate materials by precision injection molding, resulting in a smooth surface with a roughness of less than 10 μm. As shown in Fig. 1(b), each set of the NASBA primers and probes was pipetted into the designated reaction chamber and dried at room temperature. In addition, human genome DNA with a pair of primers targeting glyceraldehyde-3-phosphate dehydrogenase (GAPDH) gene was used as an internal positive control (IC). Plasmids of *Saccharomyces cerevisiae* together with the corresponding primers and probes were used as a positive control (PC) and sterilized nuclease-free water was employed as a negative control (NC). After the pre-fixing of primers, the structural layer and the cover layer were sealed together by the double-sided adhesive tape and pressed with a press machine. Each chip was individually vacuum-packed and stored at –20 °C before use.

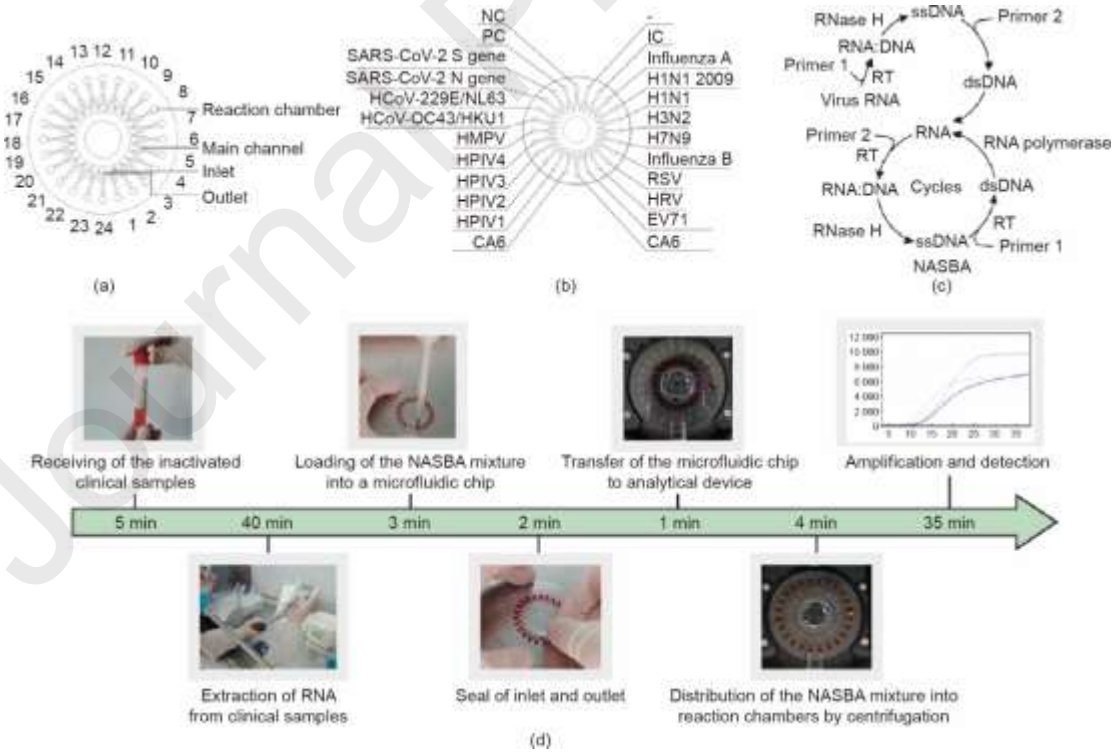

Fig. 1. Design of the disc-shaped microfluidic chip and workflow for the detection of respiratory viruses. (a) Schematic diagram of the microfluidic chip; (b) layout of the designated reaction chambers for each targeted virus and control on the chip; (c) mechanism of NASBA; in the non-cyclic phase, primer 1 anneals to the target sequence and forms an RNA:DNA hybrid. RNase H

hydrolyzes the RNA from this RNA:DNA hybrid; next, primer 2 anneals to the single-stranded DNA (ssDNA) and synthesizes a double-stranded DNA (dsDNA) by reverse transcriptase (RT); in the cyclic phase, the reaction repeats the cycles of transcription of RNA from dsDNA templates, the synthesis of cDNA, the hydrolysis of the RNA chain in the RNA:DNA hybrid, and the formation of dsDNA; (d) Workflow of virus detection. Left to right: receiving the inactivated clinical samples, extracting RNA from samples, loading reagents into the chip, sealing the chip with tape, loading the chip into the instrument, distributing reagents into the reaction chambers on the chip, and performing amplification and detection in the RTisochip^{TM}-W system.

The mechanism of NASBA is shown in Fig. 1(c) and the entire analytical process of the RTisochip^{TM}-W system is shown in Fig. 1(d). In brief, after the collection of a pharyngeal swab specimen, RNA was extracted from the clinical sample using a commercially available nucleic acid extraction kit and mixed with the reaction mixture of NASBA without primers and probes. Then, a total of 55 μL of the mixture was pipetted into the microchip through the inlet hole to fill the main channel. After that, the inlet and the outlet were sealed with two pieces of tape. Once the chip was loaded into the tray of the instrument and the start button in the control program was clicked, the rest of the procedure was carried out automatically by the system. The chip was first spun for two periods of time at a speed of 6000 rpm (rpm: revolutions per minute): first for 10 s, and then again for 30 s, after an interval of 120 s, leading to the loading of the reagents from the main channel into the 24 reaction chambers. The microfluidic chip was next incubated at 41 °C for 35 min. During this period, the fluorescence signals generated by the amplified products were detected and displayed on the computer screen in real time.

2.4. Microfluidic instrument for the analysis of respiratory infectious diseases

The RTisochip^{TM}-W consists of four identical sub-modules, each of which can control and detect a microfluidic chip. Four analyzers can be piled up to form a 16-channel system that is controlled by a single computer (Fig. 2(a)). As shown in Figs. 2(b) and (c), the sub-module is mainly composed of a motor, a control panel, a power module, a temperature-control module, a detection module, and a communication module. The control panel controls the rotation of the motor, the entry/exit of the microfluidic chip, and all the other modules. The proportional-integral-derivative (PID) temperature controller provides the temperature required for nucleic acid amplification. The optical detection system monitors the fluorescence signals in the reaction chambers in real time. Fluorescence data are sent simultaneously to the computer, which is connected with a router through the communication module.

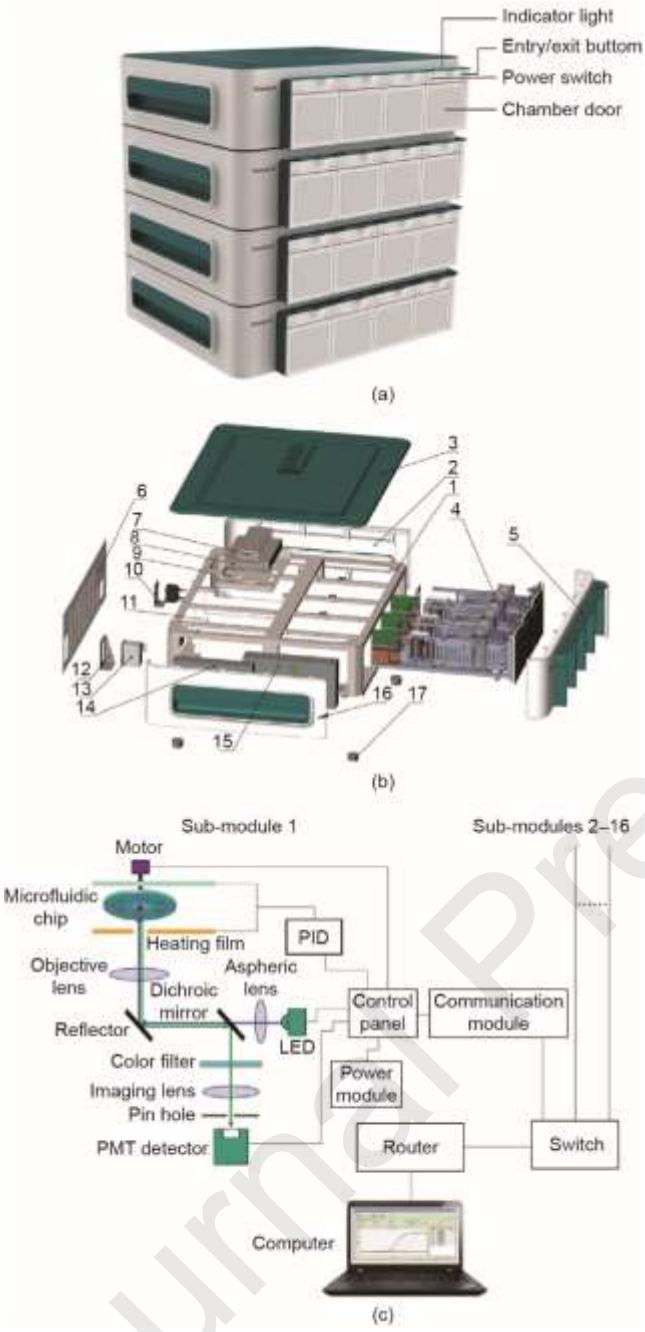

Fig. 2. Design of the RTisochip^{TM}-W system. (a) Photograph of the 16-channel RTisochip^{TM}-W with four piled analyzers, each of which contains four sub-modules; (b) exploded view of the analyzer containing four sub-modules. 1: sheet metal frame; 2: right side panel; 3: upper panel; 4: sub-module; 5: front panel; 6: rear panel; 7: fixed upper cover panel of switch; 8: switch; 9: fixed panel of switch; 10: network port mounting panel; 11: partition panel; 12: power socket mounting panel; 13: socket-type power filter; 14: power supply for the system; 15: power supply for the microchip heater; 16: left side panel; 17: rubber foot; (c) schematic of the structure of the sub-module inside the instrument. Up to 16 identical sub-modules can be connected to the computer via a router; PMT: photomultiplier tube; LED: light emitting diode.

3. Results

3.1. Optimization of RNA extractions for the RTisochip^{TM}-W system

The extraction of RNA from the clinical samples, as the first step of the analysis, plays a critical role in the entire analytical process. To select a suitable RNA extraction

method, we compared the extraction efficiencies of the TRIzol™ universal total RNA extraction kit and the QIAamp® viral RNA mini kit for the extraction of viral RNA from pharyngeal swabs. The time to a positive value (Tp), defined as the time at the second derivative inflections of the exponential amplification curves, was employed as the critical factor to evaluate the extraction efficiencies, as Tp is negatively related to the template concentration in general. As shown in Fig.3(a), we found that the Tp values provided by the TRIzol™ universal kit were always slightly shorter than those provided by the QIAamp® kit. Therefore, we chose the TRIzol™ kit as the recommended manual method for our system. Next, to further reduce the strength of manual operation, we employed the KingFisher™ Flex Purification System to automate the RNA extraction procedure. Figs. 3(b) and (c) demonstrate that this automatic system generally provided a higher extraction efficiency and better reproducibility than the manual TRIzol™ method in the detection of two viral targets, HCoV-229E/NL63 and H1N1 2009, in a wide range of virus concentrations represented by median tissue culture infectious dose ($TCID_{50}$). However, due to the higher costs of the automated system, we chose both the TRIzol™ universal kit and the KingFisher™ system for the subsequent tests.

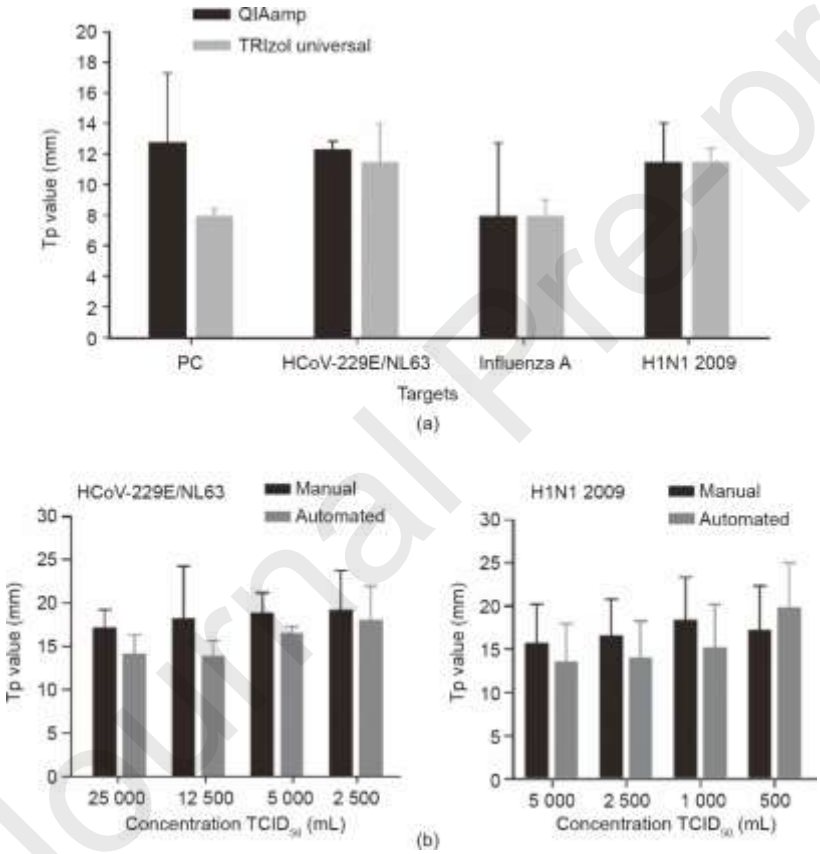

Fig. 3. Comparison of different RNA extraction methods for on-chip virus detection. (a) Comparison of the RNA extraction efficiencies of the QIAamp® and the TRIzol™ kits by detecting four different virus targets (n = 3); (b) comparison of the manual TRIzol™ kit and the automated KingFisher™ Flex Purification System in the detection of HCoV-229E/NL63 and H1N1 2009 (n = 3). All error bars represent one standard deviation.

3.2. Evaluation of the sensitivity and repeatability of the RTisochip™-W

To evaluate the sensitivity of the platform, the synthesized RNA templates of these 19 respiratory viruses were diluted to form a concentration gradient from 250, 50, 25, to 10 copies·μL^{-1}. Among them, SARS-CoV-2 N and SARS-CoV-2 S were diluted together. The limits of detection (LOD) of all the viruses are listed in Fig. 4(a). We

determined that the LODs of H7N9, CA16, RSV, HPIV1, HPIV2, HPIV3, HPIV4, HCoV-229E/NL63, and HMPV were 50 copies per microliter; that those of H1N1, H3N2, Influenza B, EV71, HCoV-OC43/HKU1, CA6, HRV, and SARS-CoV-2 N gene were 25 copies per microliter; and that those of H1N1 2009 and SARS-CoV-2 S gene could even reach 10 copies per microliter. All these results are comparable to those of the conventional RT-PCR method. Typical amplification curves of H1N1 2009 and SARS-CoV-2 S at different RNA concentrations as well as the NCs are shown in Figs. 4(b) and (c). Good linear correlations were observed between the Tp values and the RNA concentrations in H1N1 2009 and SARS-CoV-2 S gene.

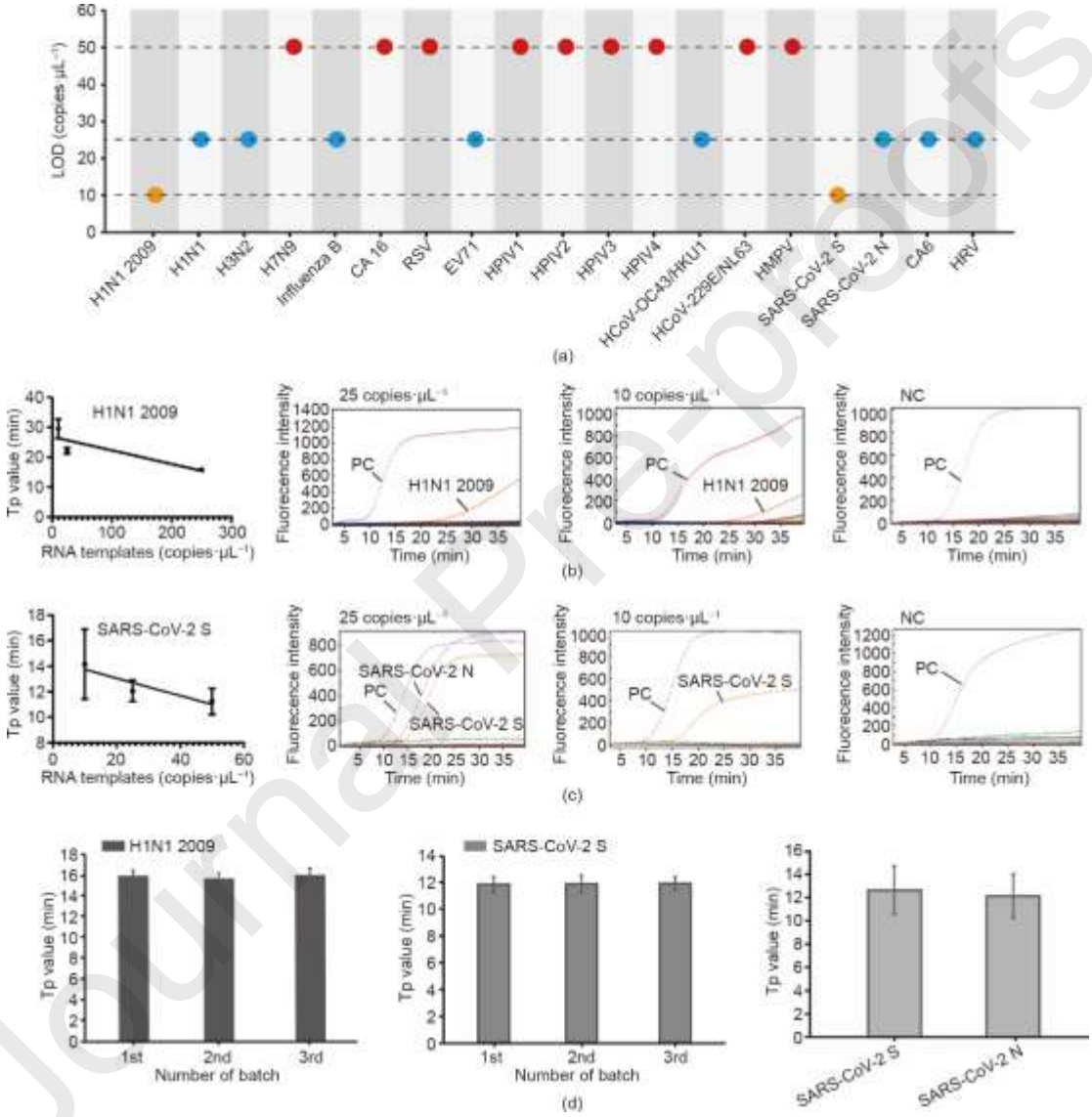

Fig. 4. Sensitivity and repeatability tests of the RTisochip^{TM}-W system. (a) LOD of 19 respiratory viruses tested by the on-chip assays; (b) typical amplification curves and linear fitting between the Tp and the template concentration of H1N1 2009 (n = 3); (c) typical amplification curves and linear fitting of SARS-CoV-2 S gene (n = 3); (d) repeatability tests of three microfluidic chips with synthesized RNA templates of H1N1 2009 and SARS-CoV-2 S gene (n = 10); (e) repeatability of the detection of SARS-CoV-2 S and N genes with extracted RNA samples (n = 10). All error bars represent one standard deviation.

We chose H1N1 2009 and SARS-CoV-2 as the detection targets for the evaluation of the system repeatability. First, three batches of the microfluidic chips (ten replicates

in each batch) were tested with the inactivated virus stocks of H1N1 2009 and SARS-CoV-2 S gene at a concentration of 500 copies per microliter. After the RNA extraction, the prepared samples were loaded into the RTisochip^{TM}-W system for testing. As shown in Fig. 4(d), no significant differences were observed in terms of the Tp values of these two targets within each batch and among three batches, indicating the excellent repeatability of our RTisochip^{TM}-W system. After the evaluation with mock samples, we further selected SARS-CoV-2 S and N genes as targets to test the repeatability with RNA extracted from clinical samples. Fig. 4(e) shows that the coefficients of variation (CV) of the S and N genes with ten repeats were 16.96% and 15.91%, respectively. These results clearly demonstrate that our microfluidic platform can provide acceptable sensitivities with high repeatability for multi-index virus detection.

3.3. Evaluation of the robustness and specificity of the RTisochip^{TM}-W system

Robustness is a crucial feature of a medical diagnostic platform, especially for the diagnosis of infectious diseases, because clinical samples may come in various forms and contain diverse amplification inhibitors that cannot be eliminated by the extraction process. In our study, the pharyngeal swabs or other types of specimens could have had multiple interferents, including microorganisms, blood, and residual antibacterial and antiviral drugs that the patients took prior to sampling. Thus, we thoroughly evaluated the anti-interference capability of our platform using samples with artificially added interferents. First, as shown in Fig. 5(a), we found that that the addition of mucin at a final concentration of 10 mg·L^{-1} into a 1×10^4 copies per milliliter virus mixture of H1N1 2009, H3N2, Influenza B, RSV, HPIV3, and SARS-CoV-2 N had no negative impacts on the amplification of these five targets, as the Tp values were not changed significantly. Next, we prepared a mixture of interfering substances, including oxymetazoline hydrochloride, dexamethasone, interferon, lamivudine, amantadine, menthol, sodium chloride, and mucoprotein (listed in Fig. 5(b)), in order to more critically evaluate the anti-interference performance of the platform. As shown in Fig. 5(c), the Tp values of H1N1 2009, H3N2, Influenza B, RSV, HPIV3, and SARS-CoV-2 N gene showed no significant changes after these mixed interferents were added. Nevertheless, these tests proved that the interferents presented in the samples had no significant negative effects on our RTisochip^{TM}-W platform.

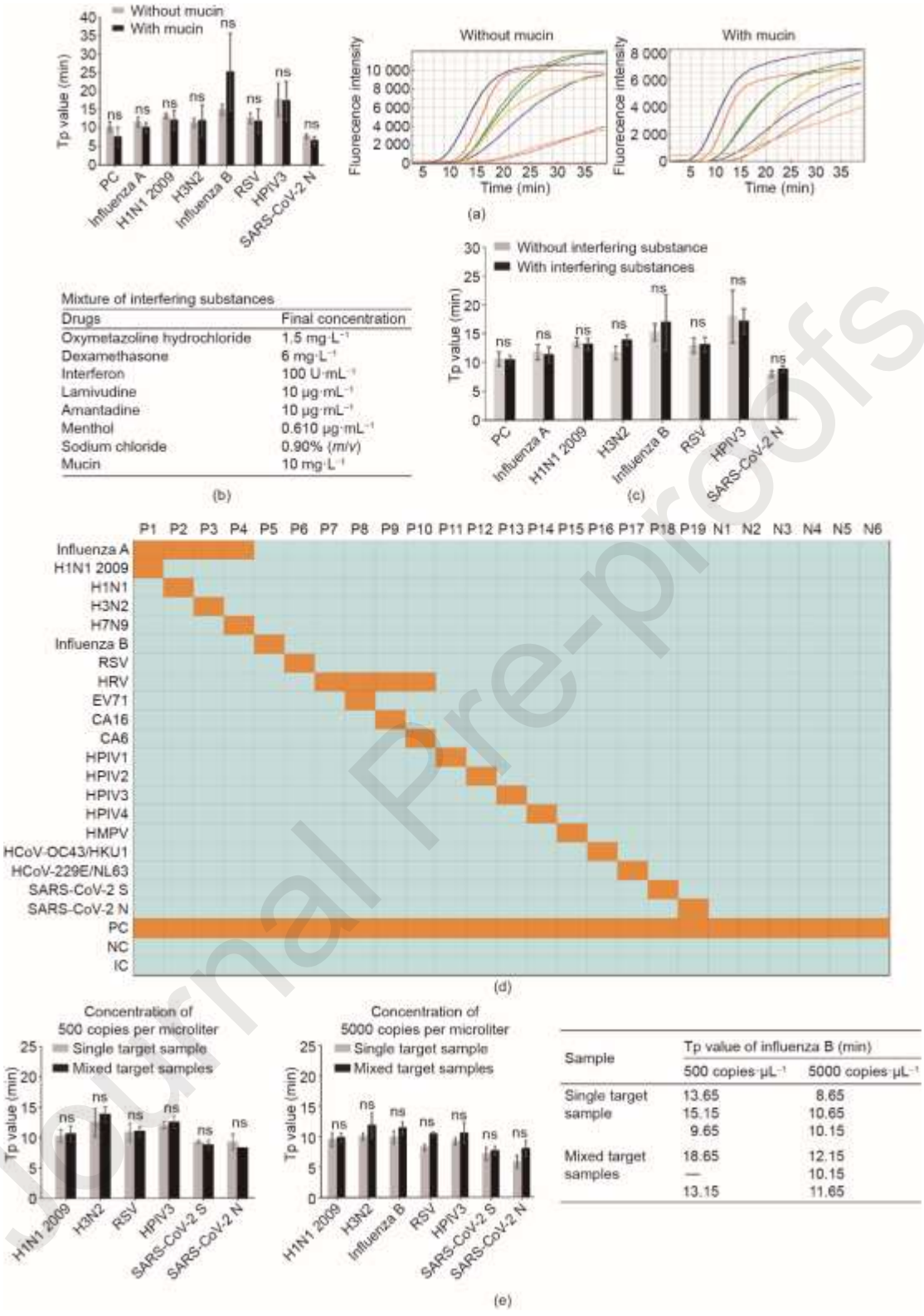

Sample	Tp value of influenza B (min)	
	500 copies·μL⁻¹	5000 copies·μL⁻¹
Single target sample	13.65	8.65
	15.15	10.65
	9.65	10.15
Mixed target samples	18.65	12.15
	—	10.15
	13.15	11.65

Fig. 5. Anti-interference, cross-reaction, and competitive effect tests of the RTisochip™-W. (a) Similar Tp values and amplification curves of seven selected targets in reactions with or without mucin; (b) final concentrations of the interfering substances added to the reaction buffer; (c) similar Tp values of seven selected targets in reactions with or without mixed interfering substances. (d) cross-reaction tests of the platform. Positive results are shown as orange squares, while azure squares represent negative results; P1–P19: virus template; N1–N6: NCs; (e) competitive effect tests of mixed target samples. Two different concentrations of single- or mixed-target samples were

tested and influenza B was missed at the low concentration of 500 copies per microliter. ns: not significant.

Since our platform can detect 19 different types of viruses simultaneously, the cross-reactions among these targets need to be thoroughly investigated, as a cross-reaction may induce false-positive results in the tests. Here, we prepared 19 samples, each of which contained a single type of virus template (P1–P19), and six NCs (N1–N6) to test our system. As shown in the heatmap of Fig. 5(d), we found that there was no non-specific amplification caused by the cross-reactions in all of the 25 samples, indicating the reliability of the RTisochip^{TM}-W system. Next, we noticed that the competitive effect within these 19 different targets is another potential risk for the platform. When multiple targets are present in a single sample, our system might be less sensitive than a system that is detecting only one target at a time, due to interference from the non-targeted RNA background. To evaluate this competitive effect, we prepared single- or mixed-RNA samples that were diluted to final concentrations of 5000 and 500 copies per microliter. As shown in Fig. 5(e), the Tp values of H1N1 2009, H3N2, RSV, HPIV3, SARS-CoV-2 S, and SARS-CoV-2 N detected individually were not significantly different from those obtained from the mixed RNA samples at the concentrations of 5000 and 500 copies per microliter. Although we did observe that influenza B was not detectable in the mixed samples at the lower concentration due to the non-targeted RNA background, the primer concentrations and primer sequences of influenza B can be further optimized to resolve this problem. Overall, the above results proved that the RTisochip^{TM}-W system possesses good specificity, strong robustness, and a powerful testing capacity for detecting 19 respiratory viruses from 16 clinical samples at the same time.

3.4. Clinical tests of SARS-CoV-2 and another 18 respiratory viruses using the RTisochip^{TM}-W

Prior to the outbreak of SARS-CoV-2, we had followed the epidemic trends of 18 types of respiratory viruses in Beijing by analyzing a large number of clinical samples using the RTisochip^{TM}-W system. During the flu season from 27 December 2019 to 16 January 2020, a total of 101 flu-season samples of children's throat swabs were collected by the Beijing Tsinghua Changgung Hospital. As a comparison, 100 non-flu-season samples of children's throat swabs were collected by the Capital Institute of Pediatrics between 18 September and 7 November 2019. All clinical samples were tested by the RTisochip^{TM}-W system; the results are listed in Tables S2–S3 of Appendix A. From these 201 clinical samples, we found that the positive rates of these respiratory viruses showed large variations over the sampling time. As shown in Fig. 6(a), almost 71.3% of the flu-season samples were found to be infected with influenza viruses, in comparison with only 2.9% of the non-flu-season samples from Capital Institute of Pediatrics. Furthermore, the positive ratios of RSV, HPIV1, HPIV2, HMPV, HCoV-229E/NL63, and HCoV-OC43/HKU1 were on the rise into the flu season. Conversely, the positive ratios of HRV, HPIV3, and HPIV4 were lower in the flu-season samples than in the non-flu-season samples. The significant changes in the positive rates of respiratory viruses over time underlined the importance of the multi-index detection of respiratory viruses in clinics.

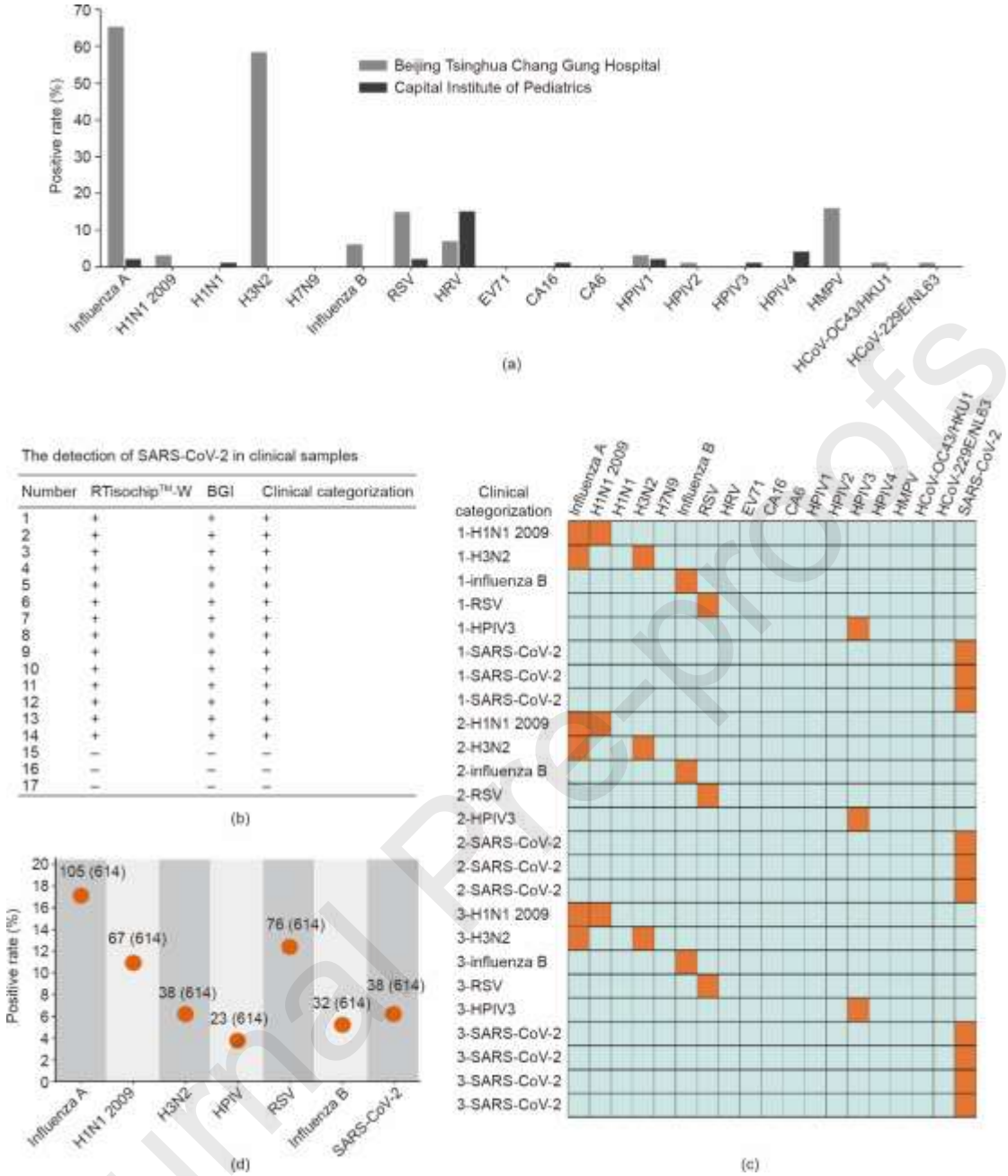

Fig. 6. Clinical identification of respiratory viruses using the RTisochip™-W. (a) Positive rates of each virus target in clinical samples collected in 2019–2020. Samples from the Beijing Tsinghua Changgung Hospital were collected in the flu season from 2019 to 2020 (n = 101), and samples from the Capital Institute of Pediatrics were collected in the non-flu season of 2019 (n = 100); (b) comparison of the SARS-CoV-2 detection results obtained by the RTisochip™-W and the conventional RT-PCR. "+" represents a positive result and "–" is negative; (c) repeatability tests of the RTisochip™-W using clinical samples. Positive and negative results are shown as orange and azure squares, respectively; (d) positive rates of a total of 614 clinical throat swab samples from suspected or confirmed COVID-19 patients. The detailed number was indicated.

After the outbreak of SARS-CoV-2, we added SARS-CoV-2 S and N genes to the system and evaluated the system performance using clinical SARS-CoV-2 samples. First, 14 clinically confirmed positive and three negative samples were tested by the RTisochip™-W system and the commercial RT-PCR kit (BGI, China) in parallel. As summarized in Fig. 6(b) and Table S4 of Appendix A, both methods showed a 100% consistency, indicating that the detection performance of our platform was the same as

that of conventional RT-PCR. To further verify the stability and repeatability of our platform for testing clinical samples, we prepared a total of 25 microfluidic chips manufactured in three different batches to test 25 clinically confirmed samples. As illustrated in the heat map in Fig. 6(c), the results reported by our RTisochip^{TM}-W system were all consistent with the clinical records, and no false-positive or false-negative results were obtained. After these small-scale evaluations, we collected a total of 614 clinical swab samples from suspected or confirmed COVID-19 patients in collaboration with the First Affiliated Hospital of Guangdong Medical College (380 cases), the West China Hospital of Sichuan University (63 cases), and the Beijing Youan Hospital of Capital Medical University (171 cases) (listed in Tables S5–S8 of Appendix A). As shown in Fig. 6(d), the positive rates of SARS-CoV-2, H1N1 2009, H3N2, HPIV, RSV, and influenza B reported by our system were 6.19% (38/614), 10.91% (67/614), 6.19% (38/614), 3.75% (23/614), 12.38% (76/614), and 5.21% (32/614), respectively. The total coincidence rates of the RTisochip^{TM}-W with the referenced kits (RT-PCR, Shanghai ZJ Bio-Tech Co., Ltd., China) in the tests of SARS-CoV-2, H1N1 2009, H3N2, HPIV, RSV, and influenza B were 98.15%, 98.70%, 99.35%, 99.57%, 97.61%, and 99.35%, respectively. In these clinical samples, some suspected COVID-19 patients were eventually diagnosed as influenza A, influenza B, or RSV instead of SARS-CoV-2. For example, case No.1 from the West China Hospital of Sichuan University was diagnosed as influenza A, highlighting the value of our platform for precisely identifying the exact cause of diseases. In some clinically confirmed COVID-19 cases, neither our platform nor conventional RT-PCR methods could detect SARS-CoV-2, probably due to the low viral loads of the samples. Such a large scale of clinical tests clearly proved that our platform is a powerful and reliable diagnostic tool in the detection of respiratory viruses in clinical settings.

4. Discussion

Since there is no effective drug for COVID-19 at present, the only feasible way to fight against COVID-19 is to diagnose, classify, and isolate patients as early as possible. Unfortunately, due to the similar symptoms of all respiratory infection diseases, it is not uncommon to find that a SARS-CoV-2-negative patient with the symptoms of cough and fever has been admitted to an intensive care unit (ICU) room with other COVID-19 patients and has been treated as having COVID-19 in a medical resource-constrained situation. From this perspective, the development of a nucleic acid testing tool for distinguishing COVID-19 from cases of pneumonia caused by other viruses—such as influenza viruses, parainfluenza virus, adenovirus, RSV, rhinovirus, and HMPV—is extremely valuable. The RTisochip^{TM}-W system is capable of identifying 19 common respiratory viruses in a single test and possesses the advantages of a short turnaround time of less than 90 min, a flexible throughput from one to 16 samples, minimum manual operations for multi-index detections, a sensitivity that is comparable to that of conventional RT-PCR, and a high tolerance for various interferents. Therefore, the RTisochip^{TM}-W system should be able to play a significant role in fighting the COVID-19 pandemic.

Application of the RTisochip^{TM}-W system in clinical practice should be elaborately planned within the context of the pandemic. Here, we present a guideline of testing for COVID-19 by comprehensively considering the pros and cons of all the molecular diagnosis methods. As shown in Fig. 7, first, when patients with COVID-19-like symptoms arrive at the fever outpatient department, a conventional RT-PCR test can be administrated to rapidly identify whether the patients (and their close contacts) have been infected with SARS-CoV-2. Due to its relatively low cost and high throughput, assisted by robotics, RT-PCR is suitable for screening a large number of

samples in a pandemic situation. If a patient is diagnosed as COVID-19, he or she could be moved to a designated COVID-19 hospital. During treatment, the viral loads of the patients can be closely monitored using digital PCR (dPCR), which can provide an absolute virus quantitation. Recent studies have shown that the viral load within the patient's body reflects the treatment outcomes [32–34]. If the patient's status deteriorates, the RTisochip^{TM}-W system can be utilized to identify the presence of any hospital-acquired infections (HAIs) caused by respiratory viruses and bacteria. This testing strategy should be able to improve the survival rate of COVID-19 patients. Second, if patients at the fever outpatient department test as negative in the SARS-CoV-2 tests, our RTisochip^{TM}-W could soon identify whether the symptoms are caused by other known viruses and bacteria in the pathogen list of the system. Once diagnosed, the patients could be moved to the pneumology department of the hospital and be closely monitored by the RTisochip^{TM}-W. Third, if the patients at the fever outpatient department still test as negative, next-generation DNA/RNA sequencing could be used to identify any unknown or uncommon pathogens. Then, the patients could be treated properly in the pneumology department and be monitored by our RTisochip^{TM}-W for any sign of HAI. Finally, the recovered patients should accept another round of RT-PCR tests before being discharged. Meanwhile, considering the possible false-negative results of RT-PCR, IgM- and IgG-based immunoassays should be coupled with RT-PCR to improve the accuracy of the test, as recommended by the Diagnosis and Treatment Protocol for Novel Coronavirus Pneumonia (trial version 7) [35].

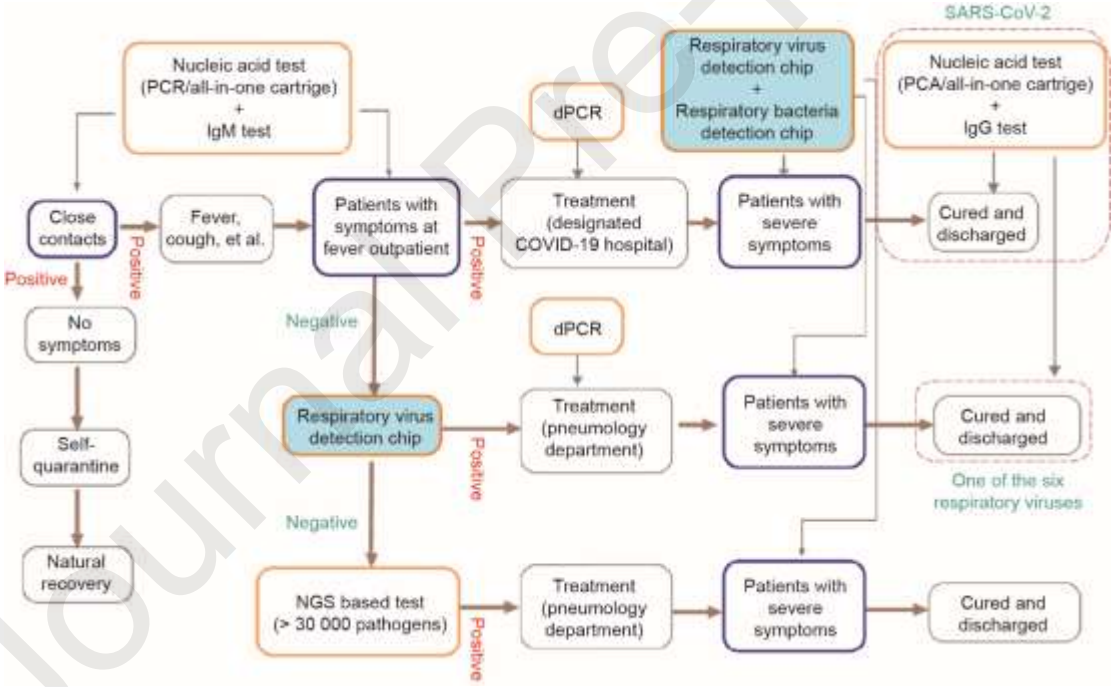

Fig. 7. COVID-19 testing guideline. NGS: next generation sequencing.

Based on this guideline, the RTisochip^{TM}-W system can be used in the following scenarios: ① to rapidly diagnose the exact cause of COVID-19-like symptoms in most cases in order to prevent mistreatment and cross-infection among patients; and ② to closely monitor the occurrence of HAIs during treatment due to the deterioration of medical situations caused by the pandemic. The RTisochip^{TM}-W system, synergistically combined with other *in vitro* diagnostic tools, will make our fight against COVID-19 more efficient and more precise. In the future, the capability of the RTisochip^{TM}-W can be further improved by introducing more pathogens into the

detection list, by integrating sample preparations to form a "sample-in-answer-out" system, and by combining with an automated robotic system to reach higher throughput.

5. Conclusion

In summary, we have successfully developed a high-throughput nucleic acid isothermal amplification system that is capable of detecting 19 common respiratory viruses, including SARS-CoV-2, from 16 clinical samples within 90 min. The high sensitivity, good specificity, strong robustness, and excellent repeatability demonstrated in the extensive clinical tests proved that our RTisochip^{TM}-W system can be utilized as a powerful nucleic acid testing tool in the diagnosis and screening of respiratory viruses, including SARS-CoV-2, in fever outpatient departments, ICUs, medical quarantine areas, and many other settings, where the precise cause of pneumonia is urgently demanded.

Acknowledgements

We thank Dr. Nanshan Zhong and his colleagues from the First Affiliated Hospital of Guangzhou Medical University for providing the inactivated virus culture stocks. We thank Dr. Xiuying Zhao and her colleagues from the Beijing Tsinghua Changgung Hospital and Dr. Xiaodai Cui and his colleagues from the Capital Institute of Pediatrics for providing clinical samples. This work is funded by the National Key Research and Development Program of China (2020YFC0847400) from the Ministry of Science and Technology of China and by the Project of Science and Technology Emergency Response for Prevention and Control of COVID-19 from the Tsinghua University.

Compliance with ethics guidelines

Wanli Xing, Yingying Liu, Huili Wang, Shanglin Li, Yongping Lin, Lei Chen, Yan Zhao, Shuang Chao, Xiaolan Huang, Shaolin Ge, Tao Deng, Tian Zhao, Baolian Li, Hanbo Wang, Lei Wang, Yunpeng Song, Ronghua Jin, Jianxing He, Xiuying Zhao, Peng Liu, Weimin Li, and Jing Cheng declare that they have no conflict of interest or financial conflicts to disclose.

Appendix A. Supplementary date

Supplementary data to this article can be found online at

References

[1] Wang C, Horby PW, Hayden FG, Gao GF. A novel coronavirus outbreak of global health concern. Lancet 2020;395(10223):470-473.
[2] Huang C, Wang Y, Li X, Ren L, Zhao J, Hu Y, et al. Clinical features of patients infected with 2019 novel coronavirus in Wuhan, China. Lancet 2020;395(10223):497–506.
[3] Corman VM, Landt O, Kaiser M, Molenkamp R, Meijer A, Chu DKW, et al. Detection of 2019 novel coronavirus (2019-nCoV) by real-time RT-PCR. Euro Surveill 2020;25(3):2000045.
[4] Chu DKW, Pan Y, Cheng SMS, Hui KPY, Krishnan P, Liu Y, et al. Molecular diagnosis of a novel coronavirus (2019-nCoV) causing an outbreak of pneumonia. Clin Chem 2020;66(4):549–55.
[5] Wilder-Smith A, Freedman DO. Isolation, quarantine, social distancing and community containment: pivotal role for old-style public health measures in the novel coronavirus (2019-nCoV) outbreak. J Travel Med 2020;27(2):taaa020.
[6] Li G, De Clercq E. Therapeutic options for the 2019 novel coronavirus (2019-nCoV). Nat Rev Drug Discov 2020;19(3):149–50.
[7] Zhai P, Ding Y, Wu X, Long J, Zhong Y, Li Y. The epidemiology, diagnosis and treatment of COVID-19. Int J Antimicrob Agents 2020;55(5):105955.
[8] Westh H, Lisby G, Breysse F, Böddinghaus B, Chomarat M, Gant V, et al. Multiplex real-time PCR and blood culture for identification of bloodstream pathogens in patients with suspected sepsis. Clin Microbiol Infect 2009;15(6):544–51.
[9] Li Y, Guo SJ, Shao N, Tu S, Xu M, Ren ZR, et al. A universal multiplex PCR strategy for 100-

plex amplification using a hydrophobically patterned microarray. Lab Chip 2011;11(21):3609–18.
[10] Wang Y, Sims CE, Allbritton NL. Dissolution-guided wetting for microarray and microfluidic devices. Lab Chip 2012;12(17):3036–9.
[11] Du W, Li L, Nichols KP, Ismagilov RF. SlipChip. Lab Chip 2009;9(16):2286–92.
[12] Shen C, Xu P, Huang Z, Cai D, Liu SJ, Du W. Bacterial chemotaxis on SlipChip. Lab Chip 2014;14(16):3074–80.
[13] Shen F, Du W, Davydova EK, Karymov MA, Pandey J, Ismagilov RF. Nanoliter multiplex PCR arrays on a SlipChip. Anal Chem 2010;82(11):4606–12.
[14] Zhukov DV, Khorosheva EM, Khazaei T, Du W, Selck DA, Shishkin AA, et al. Microfluidic SlipChip device for multistep multiplexed biochemistry on a nanoliter scale. Lab Chip 2019;19(19):3200–11.
[15] Barbulovic-Nad I, Yang H, Park PS, Wheeler AR. Digital microfluidics for cell-based assays. Lab Chip 2008;8(4):519–26.
[16] Sista R, Hua Z, Thwar P, Sudarsan A, Srinivasan V, Eckhardt A, et al. Development of a digital microfluidic platform for point of care testing. Lab Chip 2008;8(12):2091–104.
[17] Abd Rahman N, Ibrahim F, Aeinehvand MM, Yusof R, Madou M. A microfluidic Lab-on-a-Disc (LOD) for antioxidant activities of plant extracts. Micromachines 2018;9(4): 140.
[18] Stumpf F, Schwemmer F, Hutzenlaub T, Baumann D, Strohmeier O, Dingemanns G, et al. LabDisk with complete reagent prestorage for sample-to-answer nucleic acid based detection of respiratory pathogens verified with influenza A H3N2 virus. Lab Chip 2016;16(1):199–207.
[19] Hou J, Wu H, Zeng X, Rao H, Zhao P. Clinical evaluation of the loop-mediated isothermal amplification assay for the detection of common lower respiratory pathogens in patients with respiratory symptoms. Medicine (Baltimore) 2018;97(51):e13660.
[20] Hanson KE, Couturier MR. Multiplexed molecular diagnostics for respiratory, gastrointestinal, and central nervous system infections. Clin Infect Dis 2016;63(10):1361–7.
[21] Popowitch EB, O'Neill SS, Miller MB. Comparison of the Biofire FilmArray RP, Genmark eSensor RVP, Luminex xTAG RVPv1, and Luminex xTAG RVP fast multiplex assays for detection of respiratory viruses. J Clin Microbiol 2013;51(5):1528–33.
[22] Rand KH, Rampersaud H, Houck HJ. Comparison of two multiplex methods for detection of respiratory viruses: FilmArray RP and xTAG RVP. J Clin Microbiol 2011;49(7):2449–53.
[23] Compton J. Nucleic acid sequence-based amplification. Nature 1991;350(6313):91–2.
[24] Malek L, Sooknanan R, Compton J. Nucleic acid sequence-based amplification (NASBA). Methods Mol Biol 1994;28:253–60.
[25] van Gemen B, Kievits T, Nara P, Huisman HG, Jurriaans S, Goudsmit J, et al. Qualitative and quantitative detection of HIV-1 RNA by nucleic acid sequence-based amplification. AIDS 1993;7(Suppl 2):S107–10.
[26] Mugasa CM, Katiti D, Boobo A, Lubega GW, Schallig HDFH, Matovu E. Comparison of nucleic acid sequence-based amplification and loop-mediated isothermal amplification for diagnosis of human African trypanosomiasis. Diagn Microbiol Infect Dis 2014;78(2):144–8.
[27] Mercier-Delarue S, Vray M, Plantier JC, Maillard T, Adjout Z, de Olivera F, et al. Higher specificity of nucleic acid sequence-based amplification isothermal technology than of real-time PCR for quantification of HIV-1 RNA on dried blood spots. J Clin Microbiol 2014;52(1):52–6.
[28] Dimov IK, Garcia-Cordero JL, O'Grady J, Poulsen CR, Viguier C, Kent L, et al. Integrated microfluidic tmRNA purification and real-time NASBA device for molecular diagnostics. Lab Chip 2008;8(12):2071–8.
[29] Houde A, Leblanc D, Poitras E, Ward P, Brassard J, Simard C, et al. Comparative evaluation of RT-PCR, nucleic acid sequence-based amplification (NASBA) and real-time RT-PCR for detection of noroviruses in faecal material. J Virol Methods 2006;135(2):163–72.
[30] Huang G, Huang Q, Xie L, Xiang G, Wang L, Xu H, et al. A rapid, low-cost, and microfluidic chip-based system for parallel identification of multiple pathogens related to clinical pneumonia. Sci Rep 2017;7:6441.
[31] Zhang G, Zheng G, Zhang Y, Ma R, Kang X. Evaluation of a micro/nanofluidic chip platform for the high-throughput detection of bacteria and their antibiotic resistance genes in post-neurosurgical meningitis. Int J Infect Dis 2018;70:115–20.
[32] Yu F, Yan L, Wang N, Yang S, Wang L, Tang Y, et al. Quantitative detection and viral load analysis of SARS-CoV-2 in infected patients. Clin Infect Dis 2020. In press.

[33] Kim JY, Ko JH, Kim Y, Kim YJ, Kim JM, Chung YS, et al. Viral load kinetics of SARS-CoV-2 infection in first two patients in Korea. J Korean Med Sci 2020;35(7):e86.
[34] Liu Y, Yang Y, Zhang C, Huang F, Wang F, Yuan J, et al. Clinical and biochemical indexes from 2019-nCoV infected patients linked to viral loads and lung injury. Sci China Life Sci 2020;63(3):364–74.
[35] National Health Commission of the People's Republic of China; National Administration of Traditional Chinese Medicine. Diagnosis and treatment protocol for novel coronavirus pneumonia (trial version 7). Chin Med J. Epub 2020;133(9):1087–95.a